Photorefractive subharmonics—a beam-coupling effect?

Henrik C. Pedersen

Applied Optics Group, School of Physical Sciences, University of Kent, Canterbury, Kent CT2 7NR, UK

Per M. Johansen

Optics and Fluid Dynamics Department, Risø National Laboratory, DK-4000 Roskilde, Denmark

D. J. Webb

Applied Optics Group, School of Physical Sciences, University of Kent, Canterbury, Kent CT2 7NR, UK

Received September 9, 1997; revised manuscript received November 4, 1997

Using the so-called ac field technique, we investigate experimentally the influence of optical beam coupling on the generation of subharmonic gratings in a photorefractive sillenite crystal. By the use of two different recording configurations, we are able to distinguish between effects caused by material nonlinearities and effects caused by optical beam coupling. [S0740-3224(98)00305-1]

OCIS codes: 160.5320, 050.2770.

1. INTRODUCTION

Subharmonic generation in photorefractive crystals refers to the effect in which a fundamental holographic grating with a grating vector **K**, recorded in a photorefractive crystal by two crossed laser beams, becomes unstable against the excitation of new secondary gratings with grating vectors **K**/2, **K**/3, and **K**/4, etc.,[1] as illustrated in Fig. 1. The first attempts at finding an explanation for this effect were based on beam coupling,[2,3] relying on the preferential amplification in certain directions of scattered light. However, many characteristic features that were observed experimentally could not be explained by this approach. Subsequently, pure material theories were introduced[4–7] in which beam coupling is disregarded so that only the material equations (band-transport equations) are considered. From these models it was found that pairs of secondary gratings for which $\mathbf{k}_1 + \mathbf{k}_2 = \mathbf{K}$, where $\mathbf{k}_{1,2}$ are their grating vectors, can be excited spontaneously in the medium, i.e., in the absence of any $\mathbf{k}_{1,2}$ components arising from the light-interference pattern. The generation of subharmonic **K**/2, **K**/3, and **K**/4 gratings then represent special cases in which $\mathbf{k}_1$ or $\mathbf{k}_2$ assumes an integer fraction of **K**. These statements were later supported by experiments performed in a new configuration in which optical beam coupling is avoided.[8,9] There it was demonstrated that the special case of **K**/2 subharmonic generation, in which the subharmonic grating has a spatial frequency of half the fundamental one, can take place. Moreover, many other features of the experiment seemed to agree well with the space-charge wave theory.[9]

There remains, however, a fundamental feature of subharmonic generation that the space-charge wave theory has yet to explain, namely, why there seems to be a dominance of the **K**/2, **K**/3, and **K**/4 subharmonic gratings over other secondary gratings.[1,10–13] Another striking fact is that **K**/3 and **K**/4 subharmonic gratings have never been observed in the new configuration (without beam coupling). Therefore it seems natural to ask the question, Could it be that the distinct division of the secondary gratings into **K**/2, **K**/3, and **K**/4 gratings is due to beam coupling? The purpose of this paper is to elucidate this question.

Subharmomic generation has been observed in the sillenites $Bi_{12}SiO_{20}$ (BSO), $Bi_{12}TiO_{20}$, and $Bi_{12}GeO_{20}$, and two different techniques have been used: (i) application of a constant (dc) electric field via the electrodes shown in Fig. 1 along with illumination by a moving light-interference pattern (obtained by shifting the frequency of one of the optical beams),[1,8–12] and (ii) application of an alternating (ac) electric field along with illumination by a stationary light pattern.[13] In this paper we use the ac technique because with this technique the thresholds for generating the **K**/3 and **K**/4 subharmonic gratings are lower than for the dc technique; hence the **K**/3 and **K**/4 gratings are easier to excite with the ac technique. The crystal used is a BSO crystal cut so that both the traditional configuration (with beam coupling present) and the new configuration (without beam coupling) can be applied. By comparing the results of the two configurations, we are able to assess the influence of optical-beam coupling. The details of the experiments are presented in Sections 2 and 3, and the results are discussed as a whole in Section 4.

2. EXPERIMENTS PERFORMED IN THE TRADITIONAL CONFIGURATION

In the first experiment we use the configuration traditionally used in subharmonic experiments.[1,10–19] The details

0740-3224/98/051528-05$15.00

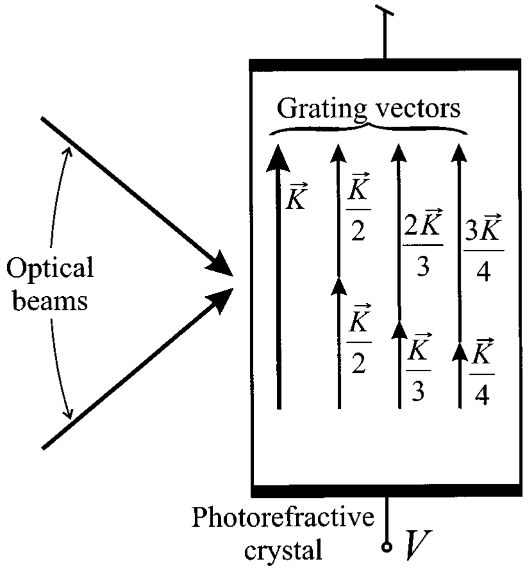

Fig. 1. Schematic diagram of subharmonic generation in a photorefractive crystal. V is the voltage applied to the crystal.

of the setup used are shown in Fig. 2. A vertically (∥ y axis), linearly polarized laser beam from a diode-pumped, frequency-doubled ND:YAG laser at wavelength 532 nm (L_1) is expanded to obtain a cross-sectional area that is large enough to cover the (110) face of the BSO crystal. A beam splitter splits the beam in two, one half of which is sent through a λ/2 plate and then via mirror M_1 to the (110) face of the crystal. The other beam is sent to the crystal via mirrors M_2 and M_3 so that the fringe spacing of the light-interference pattern is $\Lambda = 21\ \mu$m. The total intensity of the two recording beams is 40 mW/cm^2, and the beam ratio β is 2.7. By rotating the λ/2 plate, one can vary the intensity modulation m according to the formula $m = 2\sqrt{\beta}(1 + \beta)^{-1}|\cos(\theta)|$, where θ is the angle between the directions of polarization of the recording beams.

The BSO crystal is the same as that used in Ref. 8. It measures 5 mm × 10 mm × 11 mm along the $\langle 1\bar{1}0\rangle$, $\langle 110\rangle$, and $\langle 001\rangle$ crystallographic directions, respectively. The two $(1\bar{1}0)$ faces are painted with silver paint and then connected to an electric square-wave field generator, which can supply a field with an amplitude, E_{ac} as high as 7.5 kV/cm. The slew rate of the generator is 0.6 kV/μs, so that a good square-wave form can be obtained well into the kHz region.

Finally, the recorded holograms are read out by a 2-mW expanded He–Ne laser beam, which has a diameter of ~3 mm. The read-out angle of this beam is adjusted to Bragg match the fundamental grating with a grating vector **K**. The diffraction patterns are monitored on the screen S, as illustrated in Fig. 2. The reason that the read-out beam is expanded is to keep it from playing any active role in the recording process. One can easily confirm this by quickly switching on the read-out beam and then observing whether the diffraction pattern exhibits a transient change. If the pattern appears instantaneously, the read out is nondestructive.

In the first experiment the square-wave amplitude E_{ac} is set to 7.5 kV/cm, and the square-wave frequency f is set to 180 Hz. The intensity modulation coefficient is then varied by rotation of the λ/2 plate, and the resulting diffraction patterns that appear on the screen are recorded by a CCD camera. The diffraction patterns are shown in Fig. 3. At $m = 0.08$ a weak and rather broad diffraction pattern appears between the zeroth- and first-order diffraction spots. It implies that some structure with a range of grating vectors around **K**/2 is excited. By in-

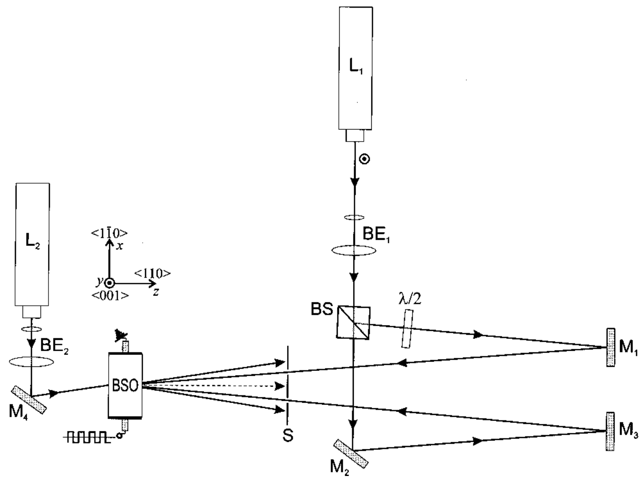

Fig. 2. Experimental setup for the traditional configuration. L_1, frequency doubled, diode pumped ND:YAG laser emitting light at 532 nm; L_2, He–Ne laser emitting light at 633 nm; BE's, are beam expanders; BS, beam splitter; λ/2, half-wave plate; M's mirrors; S, screen.

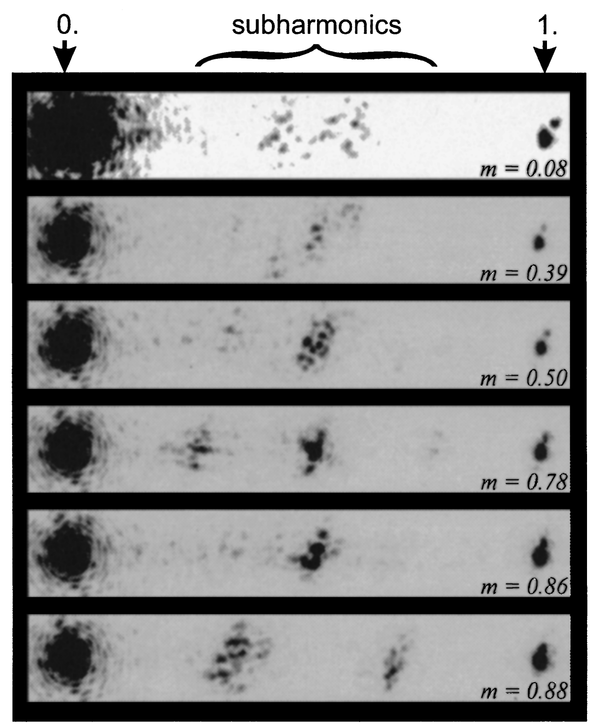

Fig. 3. Diffraction patterns obtained at the screen in the traditional configuration. The large spot on the left is due to the directly transmitted read-out beam (zeroth order), the spot on the right is due to diffraction in the fundamental grating with grating vector **K** (first order), and the light patterns between are due to diffraction in secondary gratings with grating vectors between **0** and **K**. Note that the contrast has been increased in the upper picture to be able to visualize the weak subharmonic pattern.

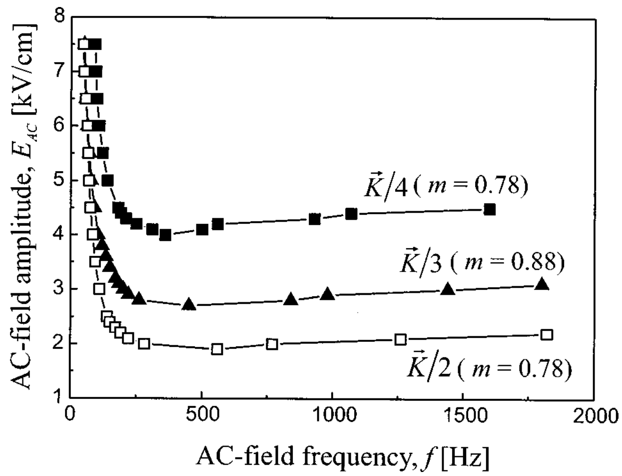

Fig. 4. Threshold values of f and E_{ac} for the different subharmonic gratings. The **K**/2 and **K**/4 curves are obtained at $m = 0.78$, whereas the **K**/3 curve is obtained for $m = 0.88$.

creasing the modulation coefficient, we see that the central diffraction pattern becomes stronger, and at $m = 0.5$ a somewhat more confined spot is observed at **K**/2. At $m = 0.78$ this central spot is even more localized, so that a more or less distinct **K**/2 grating is present, and in addition two spots appear centered at **K**/4 and 3**K**/4. At $m = 0.86$ these additional spots disappear, and at $m = 0.88$ the central spot also disappears. Instead, two new spots at **K**/3 and 2**K**/3 appear. Hence from $m = 0.78$ to $m = 0.88$ we observe a transition from mixed **K**/2, **K**/4 through pure **K**/2 to pure **K**/3 subharmonic generation. To the best of our knowledge, such a dependency on intensity modulation has never been observed before. Having said that, however, one has to add that even though the grating vectors **K**/2, **K**/3, **K**/4, etc., seem to characterize the diffraction patterns, their diffraction spots are certainly not as well defined as the one for the fundamental grating.

In Ref. 13 the transitions between different subharmonic regimes were observed when the frequency f was changed. To check whether this is the case in our experiment, too, we keep the modulation fixed and then change both f and E_A, one after the other. Surprisingly, we observed that practically nothing happens to the shape of the secondary diffraction patterns when these two parameters are varied; the patterns vary only in intensity. Thus, in our experiment, the structure of the secondary gratings, i.e., whether **K**/2, **K**/3, or **K**/4 dominates, seems to be determined by the intensity modulation, whereas the strengths of the gratings seem to be controlled by f and E_{ac}. The threshold values for f and E_{ac} are shown in Fig. 4. For all three cases it is seen that there is an upper and lower threshold for f and only a lower threshold for E_{ac}. The threshold values of E_{ac} are significantly increased as f falls below 200 Hz. It is also seen that **K**/2 has a lower threshold than **K**/3, which then again has a lower threshold than **K**/4.

3. EXPERIMENTS PERFORMED IN THE NEW CONFIGURATION

The experimental setup for the new configuration is almost identical to the one shown in Fig. 2. However, the recording beams are now incident on the crystal from above, i.e., on the (001) face, as shown in Fig. 5. This change in geometry is performed simply by tilting the two mirrors M_1 and M_3 (Fig. 1) so that the recording beams just pass the top of the crystal. By means of a new mirror M_5 (Fig. 5) positioned just above the crystal, the two beams are redirected to hit the top crystal face, (001). Thus, if we disregard the small power loss in the reflecting mirror M_5, we can assume that the fringe spacing and the dc light intensity is unchanged as compared with the traditional setup used in Section 2.

With f and E_{ac} set to 180 Hz and 7.5 kV/cm as in Fig. 3, we observe the read-out patterns shown in Fig. 6. The difference between the results obtained from the two configurations is seen immediately when these pictures are compared with the corresponding upper ($m = 0.08$) and lower ($m = 0.88$) pictures in Fig. 3. In the new configuration one sees only a line of diffracted light that more or less covers the whole distance from the zeroth- to the first-order spot. The line of light is, however, slightly filamented, apparently in some random way. In terms of structure, this pattern remains more or less the same for all values of m between 0.08 and 0.88; the only thing that changes is the intensity of the pattern, where, obviously, the intensity increases with m. As regards the dependence on f and E_{ac}, one sees a similar behavior, namely, that the structure of the diffraction pattern remains the same, but the intensity increases with f and E_{ac}. Hence in the new configuration there is no sign of any division of the secondary gratings into subharmonic gratings.

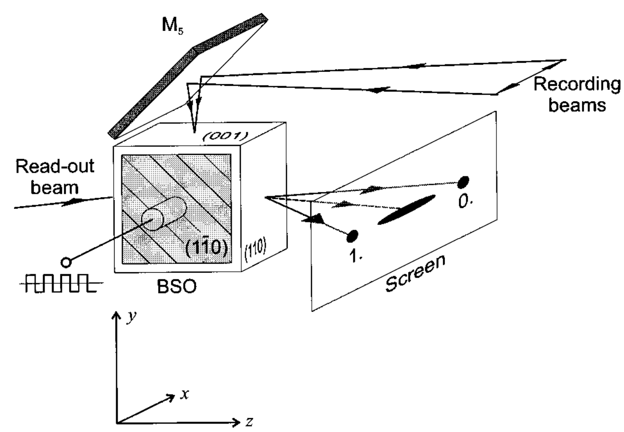

Fig. 5. Central part of the setup for the new configuration.

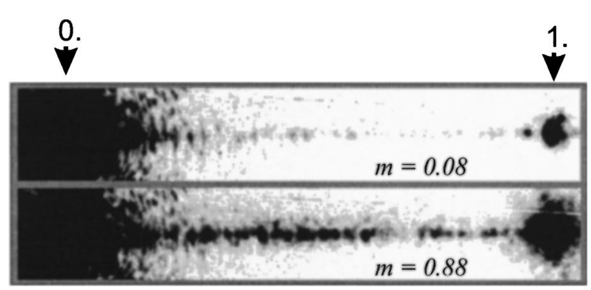

Fig. 6. Diffraction patterns obtained at the screen in the new configuration.

4. DISCUSSION

We have investigated the generation of secondary gratings in a BSO crystal under application of an ac square-wave electric field for two different configurations referred to as traditional and new. The only difference between the two is that optical beam coupling between the recording beams is possible in the traditional configuration but not in the new configuration. As regards the structure of the secondary gratings, we observe significant differences between the two configurations. In the traditional one it is possible to obtain more or less distinct subharmonic gratings, such as **K**/2, **K**/3, and **K**/4, but in the new configuration gratings with an almost continuous spectrum of grating vectors between **0** and the fundamental grating vector **K** are observed. Thus in the new configuration it is not possible to obtain distinct subharmonic generation. On the basis of these observations we can say that, when the ac technique is used, subharmonic generation, i.e., the division of the secondary gratings into **K**/2, **K**/3, **K**/4, etc., gratings, is a beam-coupling phenomenon because the divisions are seen only when beam coupling is present. What starts the subharmonic generation in the traditional configuration might, however, still be the nonlinearities in the material equations. So, what happens is, perhaps, that a broad continuum of gratings with grating vectors between **0** and **K** are excited initially through a nonlinear material process, and then beam coupling starts playing a role and favors some distinct grating vectors (**K**/2, **K**/3, **K**/4), making the final result subharmonic generation.

The broadness of the secondary diffraction spots in Fig. 3 reveals, however, that not even in the traditional configuration can one talk about pure subharmonic generation. It is more correct to speak about packages of secondary gratings with grating vectors around **K**/2, **K**/3, **K**/4, etc., rather than distinct subharmonic gratings.

The observations above are very important for future work in the field of photorefractive subharmonic generation. As regards experiments, if one intends to verify the results of the space-charge wave theory, one has to use the new configuration to avoid the influence of beam coupling. On the other hand, as regards theory, if one intends to find a theoretical explanation of subharmonic generation, one cannot restrict the analysis to the band-transport equations; beam coupling, i.e., the optical wave equation for the recording beams, has to be taken into account as well. Furthermore, because of the broadness of the secondary diffraction spots in Fig. 3, one has to consider packages of gratings with grating vectors around the subharmonic ones rather than distinct subharmonic gratings. As regards theoretical modeling of the generation of secondary gratings in the absence of beam coupling, the present space-charge wave theory seems to need modification, too, because the theory in its present form[7] considers only one distinct pair of secondary gratings. Obviously, as shown in Fig. 6, this is far from sufficient.

Most work on subharmonic generation—theoretical and experimental—concerns the dc technique (with a moving light pattern and a dc electric field). Therefore one of the very interesting questions to be investigated in the future is, Do the dc subharmonics exhibit features similar to those found here for the ac subharmonics? Our guess can only be that optical beam coupling has some influence in the dc case, too, as has been suggested already in the literature.[14,15] What is worth noting is that little emphasis has been made in investigating whether the subharmonic diffraction patterns were due to distinct gratings or narrow packages of gratings. In many cases[1,10,13,16–19] a lens has been used to focus the diffracted beams, thus making it impossible to judge their structure. Another interesting question is, Were the diffraction efficiencies of the subharmonic **K**/2 grating, obtained previously in the new configuration,[8,9] really a result of a single **K**/2 grating, or was it a narrow wave package centered at **K**/2? This question is important, as all theoretical modeling using the space-charge wave theory is based on the assumption that the subharmonic gratings are distinct and not packages.

ACKNOWLEDGMENTS

H. C. Pedersen and P. M. Johansen were supported by the Danish Natural Science Research Council, grants 9502764 and 9600986. Financial support of INTAS project 96-0954 is also gratefully acknowledged.

REFERENCES

1. S. Mallick, B. Imbert, H. Ducollet, J.-P. Herriau, and J.-P. Huignard, "Generation of spatial subharmonics by two-wave mixing in a nonlinear photorefractive medium," J. Appl. Phys. **63**, 5660–5663 (1988).
2. K. H. Ringhofer and L. Solymar, "New gain mechanism for wave amplification in photorefractive materials," Appl. Phys. Lett. **53**, 1039–1040 (1988).
3. K. H. Ringhofer and L. Solymar, "Three-wave and four-wave forward mixing in photorefractive materials," Appl. Phys. B **48**, 395–400 (1989).
4. L. B. Au, L. Solymar, and K. H. Ringhofer, "Subharmonics in BSO," in *Technical Digest on Photorefractive Materials, Effects and Devices II* (Société Francais d'Optique, Aussois, France, 1990), pp. 87–91.
5. B. I. Sturman, M. Mann, J. Otten, K. H. Ringhofer, and A. Bledowski, "Subharmonic generation in photorefractive crystals: application of theory to experiment," Appl. Phys. A **55**, 55–60 (1992).
6. B. I. Sturman, A. Bledowski, J. Otten, and K. H. Ringhofer, "Spatial subharmonics in photorefractive crystals," J. Opt. Soc. Am. B **9**, 672–681 (1992).
7. B. I. Sturman, M. Mann, J. Otten, and K. H. Ringhofer, "Space-charge waves in photorefractive crystals and their parametric excitation," J. Opt. Soc. Am. B **10**, 1919–1932 (1993).
8. T. E. McClelland, D. J. Webb, B. I. Sturman, and K. H. Ringhofer, "Generation of spatial subharmonic gratings in the absence of photorefractive beam coupling," Phys. Rev. Lett. **73**, 3082–3084 (1994).
9. B. I. Sturman, T. E. McClelland, D. J. Webb, E. Shamonina, and K. H. Ringhofer, "Investigation of photorefractive subharmonics in the absence of wave mixing," J. Opt. Soc. Am. B **12**, 1621–1627 (1995).
10. D. J. Webb and L. Solymar, "Observation of spatial subharmonics arising during two-wave mixing in BSO," Opt. Commun. **74**, 386–388 (1990).
11. P. Buchhave, S. Lyuksyutov, and M. Vasnetsov, "Relations between spontaneously occurring beams in bismuth silicon oxide with two frequency-detuned pump beams," Opt. Lett. **20**, 2363–2365 (1995).

12. P. Buchhave, S. Lyuksyutov, M. Vasnetsov, and C. Heyde, "Dynamical spatial structure of spontaneous beams in photorefractive bismuth silicon oxide," J. Opt. Soc. Am. B **13**, 2595–2601 (1996).
13. J. Takacs and L. Solymar, "Subharmonics in $Bi_{12}SiO_{20}$ with an applied ac electric field," Opt. Lett. **17**, 247–248 (1992).
14. C. H. Kwak, S. Shim, and E. H. Lee, "Coupled wave analysis of spatial subharmonics in photorefractive $Bi_{12}SiO_{20}$ crystal," Electron. Lett. **30**, 2063–2064 (1994).
15. P. M. Johansen, R. S. Hansen, and T. Olsen, "Experimental characteristics of spatial subharmonics in BSO," Opt. Commun. **115**, 308–314 (1995).
16. D. J. Webb, L. B. Au, D. C. Jones, and L. Solymar, "Onset of subharmonics generated by forward interactions in $Bi_{12}SiO_{20}$," Appl. Phys. Lett. **57**, 1602–1604 (1990).
17. C. H. Kwak, J. Takacs, and L. Solymar, "Spatial subharmonic instability in photorefractive $Bi_{12}SiO_{20}$ crystal," Elec. Lett. **28**, 530–531 (1992).
18. J. Takacs, M. Schaub, and L. Solymar, "Subharmonics in photorefractive $Bi_{12}TiO_{20}$ crystals," Opt. Commun. **91**, 252–254 (1992).
19. C. H. Kwak, J. Takacs, and L. Solymar, "Spatial subharmonic instabilities," Opt. Commun. **96**, 278–282 (1993).